THE ASTRONOMICAL JOURNAL VOLUME 113, NUMBER 1 JANUARY 1997

RY PERSEI: AN EARLY-TYPE INTERACTING CLOSE BINARY

EDWARD C. OLSON

Department of Astronomy, University of Illinois, 1002 W. Green Street, Urbana, Illinois 61801
Electronic mail: olsomed@sirius.astro.uiuc.edu

MIREK J. PLAVEC

Department of Physics and Astronomy, University of California, Los Angeles, California 90095-1562
Electronic mail: plavec@bonnie.astro.ucla.edu

Received 1996 August 24; revised 1996 September 19

ABSTRACT

We have analyzed photometric and spectroscopic data for the totally-eclipsing binary RY Persei. It is a semidetached binary of the Algol type. However, both the gainer (B4: V) and the loser (F7: II-III) are significantly more massive (6.25 and 1.6 $M_\odot$), hotter, and more luminous (M_{bol} about -3.3 and -0.2 mag, respectively) than a typical Algol system. As a possible result, the ionization level indicated by emission lines observed in the UV during total eclipse is unusually high. These lines also show evidence of CNO processing of circumstellar matter: the C IV and C II lines are weak compared to the very strong N V line. V,B photometric solutions are quite satisfactory, if the rapid rotation of the gainer (about 10 times the synchronous rate) is taken into account. On the contrary, *IUE* spectra show circumstellar structures in both continuum and absorption lines (and in emission lines in deep eclipse). RY Per straddles the border between permanent and transient accretion disks; it may be better to speak about a pseudo-photosphere. Because of its distance (about 840 pc) and low galactic latitude ($-10.5°$), interstellar extinction is appreciable; our estimate is $E(B-V)\approx 0.18$ mag. © *1997 American Astronomical Society.* [S0004-6256(97)00301-4]

1. INTRODUCTION

RY Persei (HD 17034; coordinates for 2000.0: $\alpha = 02^h\ 45^m\ 42.06^s$, $\delta = +48°\ 08'\ 37.2''$; $V \approx 8.6$ mag) is a semidetached eclipsing binary of the Algol type. That is, the less massive and cooler component (the loser) appears to be more evolved and fills its critical Roche lobe, while the more massive and hotter component (the gainer) appears to be a little evolved main-sequence star. As is normal for the entire class of Algol-type binaries, the loser was originally the more massive and more evolved component, and the present configuration is the result of massive mass transfer between the components.

RY Per is not a run-of-the-mill member of the Algol family. The gainer spectral type is significantly earlier than in most other Algol binaries; that the system is totally eclipsing makes it almost unique among those earlier-type binaries. Total eclipses yield evidence for a fairly large amount of circumstellar matter associated with mass transfer.

Perhaps because of its relatively long period, near 7 days, RY Per was long neglected by photometrists. Although it was discovered as early as 1906 (by Mme Ceraski in Moscow), its first photoelectric photometry was published by Popper & Dumont (1977), from whose observations Van Hamme & Wilson (1986, VHW) obtained photometric solutions. Spectroscopic observations were made by Hiltner (1946), and revealed a serious discrepancy between radial velocities derived from the hydrogen and helium lines. Radial velocity studies were significantly improved by Popper (1989).

IUE observations by Plavec (reported in a preliminary fashion in Plavec 1987, 1989) and by Polidan (Polidan & Wade 1992) revealed a fairly rich circumstellar emission-line spectrum in the ultraviolet, observed during the total eclipse of the system. More recently, Dr. Geraldine Peters with Plavec as Co-I obtained a set of valuable high-dispersion *IUE* spectra, which reveal corresponding circumstellar absorptions at phases outside totality. These extensive observations have not been used here as they will be discussed in a later article.

2. OBSERVATIONS

Observations used in the present study include the photometric observations of Popper and Dumont kindly provided by Dr. Popper, and Plavec's spectroscopic observations. Except for a few gaps in primary eclipse (especially during egress), photometric coverage is excellent. Spectroscopic data consist of a pair of high-dispersion *IUE* spectra (taken in the SWP and LWP cameras), a richer set of pairs of low-dispersion spectra, as well as optical spectra taken with the Lick 3 m Shane telescope. Optical spectra are of two kinds: low-dispersion IDS scans, and high-resolution CCD spectra taken with the Hamilton spectrograph. These spectra cover the wavelength interval 1200–8000 Å with a gap between about 3100 and 3500 Å, and another near-gap between about 2000 and 2300 Å, where the sensitivity of the LWP camera is poor.

An unfortunate but unavoidable aspect of this material is that data could not be obtained nearly simultaneously; obser-

 0004-6256/97/113(1)/425/8/$10.00

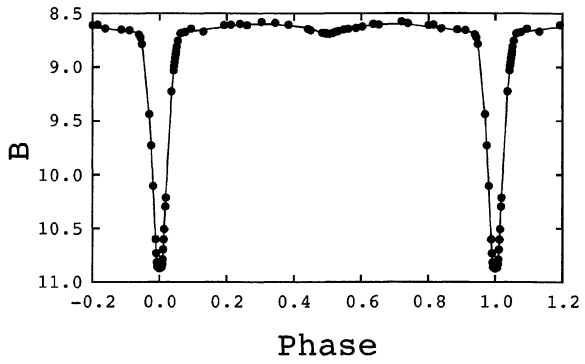

FIG. 1. Observed B normals (filled circles) and the best $[V, B]$ solution (continuous curve).

vations are scattered from 1978 through 1990, in addition to the Popper-Dumont photometry from 1972!

3. PHOTOMETRIC SOLUTIONS

Earlier simultaneous $[V,B]$ photometric solutions based on the Popper-Dumont observations were published by VHW. These investigators noted "counter intuitive kinds of solution behavior" and that "at least several local solutions" complicated interpretations. They used the now outdated model atmosphere grid of Carbon & Gingerich (1969). We therefore obtained new solutions, searching carefully for false solutions representing local, not global, error minima in parameter space.

We used the Wilson (1979, 1992) eclipsing binary modeling program with a 50×50 integration grid to obtain photometric solutions of RY Per. Following Wilson's recommendation, we obtained solutions simultaneously with V and B observations (investigating U solutions later). Stellar atmosphere subroutines of Stagg (1992) based on the Kurucz (1979) grid, and fluxes supplied by Dr. Gene Milone based on the Kurucz (1992) grid, were both used in the Wilson program.

We binned the Popper-Dumont V, B, and U observations into 84 running normals in each color. Each normal contains 3 to 14 individual observations confined to single nights or parts of nights. In the program, normals were further weighted proportional to f^{-2}, where f is the observed flux.

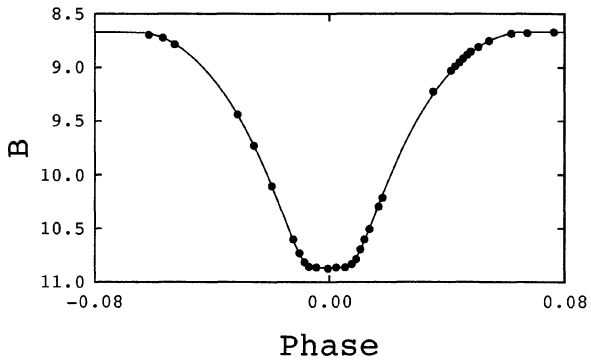

FIG. 2. Fig. 1, expanded to show primary eclipse.

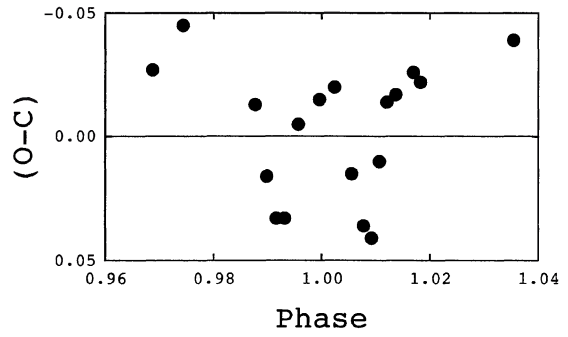

FIG. 3. B (O−C)s (mag) from the $[B,V]$ solution with rotational parameter $F_1=1.0$ (synchronous gainer rotation).

We checked one solution using unbinned observations and found virtually no parameter changes, so binning has not influenced solutions. B normals are plotted (filled circles) against orbital phase in Figs. 1 and 2.

Primary eclipse is very nearly symmetrical. We found a slight shift in the time of mid-eclipse, derived a new value, HJD=2441655.780±0.001, and combined it with the period derived by VHW; thus phases are computed using the ephemeris

$$T_0=\text{HJD } 2441655.780+6.863569\ E.$$

The semi-duration of total eclipse is (0.0069 ±0.0001)P=1.14 hrs in all colors, though in U the light curve minimum appears slightly more rounded.

We assumed the semidetached configuration for RY Per (MODE 5 of the Wilson program) and later verified it by showing that slightly detached (MODE 2) solutions yield poorer results. With the semidetached configuration, q(phot) is a proxy for the loser potential Ω_1 and loser radius.

Solutions were obtained as follows. Loser luminosities L_2 and mean temperature T_2 are first coupled (control integer $IPB=0$). Inclination i, T_2, Ω_1, photometric mass ratio (loser/gainer) q(phot), and L_1 are varied. Model atmosphere subroutines calculate L_2 at all solution wavelengths.

Parameters are affected by errors in model atmosphere fluxes and mismatches between assumed and actual filter transmissions. Improved solutions are sought by adjusting luminosities independent of model atmosphere constrains. L_2 and T_2 are decoupled ($IPB=1$). The influence of T_2 then

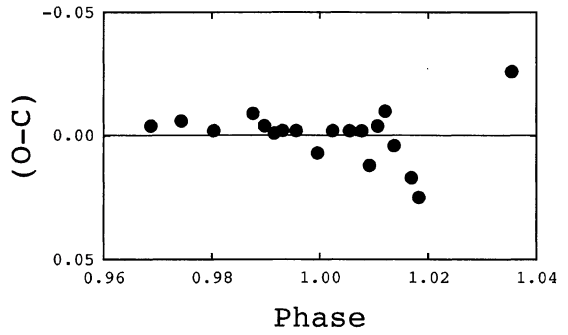

FIG. 4. Residuals as in Fig. 3, with $F_1=10$.

enters solutions weakly, through interactions. Luminosities of both stars, as well as i, Ω_1, and q(phot), are adjusted. This step is equivalent to combining separate solutions at each wavelength, with imposed common geometrical parameters and with observations properly weighted. Both radiative and geometrical parameters change, but these changes are significantly reduced with the newer Kurucz grid.

Finally, T_2 from the first coupled solution is improved. L_2 and T_2 are recoupled, the updated geometrical parameters are adopted, and only T_2 is varied.

In most solution iterations, the following parameters were fixed: mean gainer temperature T_1; gravity brightening g; bolometric albedo A; rotational parameter F (ratio of actual to synchronous rotation); linear limb-darkening x; and constant third light ℓ_3. Synchronous loser rotation was assumed ($F_2=1$). Limb-darkening parameters were taken from Van Hamme (1993). Gravity-brightening coefficients and bolometric albedos were initially set to the usual values for radiative gainer and convective loser; loser coefficients were adjusted in separate iterations. Third light was zero in all iterations.

We considered CCD high-dispersion spectra, evolutionary tracks, and polar brightening in selecting T_1 (see discussion below). The adopted value of 18,000 K is uncertain by as much as 1000 K; this uncertainty contributes significantly to parameter errors.

We explored simultaneous $[V,B]$ and $[V,B,U]$ solutions; including U observations changes solutions somewhat. U-only solutions, using the geometry of the $[V,B]$ solution, reveal effective radius differences in one, or both, stars in the ultraviolet. One might expect Roche geometry to define the maximum loser radius; accretion onto the gainer could change its effective radius in the ultraviolet. The U light curve is probably affected by circumstellar effects.

The warning of VHW about several local solutions led us to search parameter space for non-global error minima. As VHW remarked, most solution difficulties stem from attempts to include F_1 in iterations. We proceeded as follows:

The gainer in RY Per is spectroscopically a rapid rotator (Etzel & Olson 1993), so F_1 is greater then 1. Rapid rotation affects light curves mainly in primary eclipse, through the altered shape and emergent intensity distribution of the gainer. Attempts to include F_1 in $[V,B]$ solution iterations produced huge, unrealistic increments for initial values between 1 and 5. We therefore obtained a series of converged solutions with F_1 fixed at a series of values from 1 to 12. By pursuing complete solutions at each rotation, we explored all the relevant parameter space. A fairly well-defined minimum

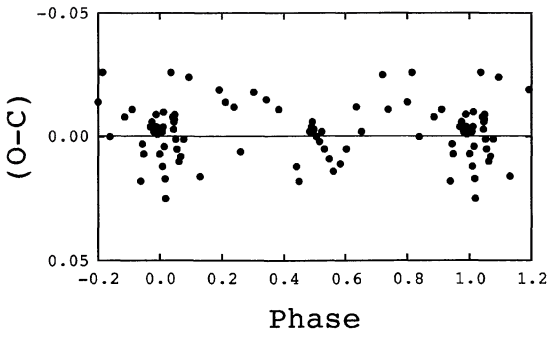

FIG. 5. Observed−computed B magnitudes from the best $[V,B]$ solution.

in SR (the sum of the squared light residuals) was found for F_1 near 10. Later decoupled iterations, including F_1 with initial values near 10, did converge successfully. As expected, solutions with $F_1=1$ and 9.8 (the best iterated value) differ significantly in primary eclipse (see Figs. 3 and 4). We did similar parameter space explorations with i, Ω_1, and q(phot). In each case, minima in SR corresponded to iterated solution values, confirming correct solution convergence.

The quality of a solution is easily judged in a plot of observed *minus* calculated (O−C) magnitude residuals. Figure 5 shows (O−C)s for B from the simultaneous $[V,B]$ solution (V residuals are similar). Small systematic residual trends are present outside primary eclipse, though they are somewhat smaller than those found by VHW. Mean residuals are about ± 0.01 mag in both V and B.

$[V,B]$ solution details are given in Tables 1 and 2. The spectroscopic mass ratio q(spec) is uncertain, because the low-amplitude gainer velocity curve is distorted by circumstellar and loser contamination. As already noted, the photometric mass ratio q(phot) is a proxy for the loser gravitational potential or radius. The formal mean error in q(phot) is ± 0.004. This value applies only if the loser photosphere exactly fills its Roche lobe and there are no other error sources (see below).

If the loser were *very* slightly detached, then an *imposed* semidetached solution would give an incorrect photometric mass ratio q_e. We obtained q_es by imposing the semidetached configuration on the series of slightly detached MODE 2 solutions mentioned above. SR increases much more rapidly with changes in q_e than it does with changes in q(phot) in the true semidetached state. Thus, very slight lobe underfilling, while possibly contributing to the error in q(phot), cannot appreciably affect photometric solutions of

TABLE 1. Wavelength-independent parameters.[a]

T_1	18000 K	g_1	1.00[b]	F_1	9.8	$r_1(pole)$	0.121	$r_2(pole)$	0.250
T_2	6250 K	g_2	0.53	F_2	1.0[b]	$r_1(pnt)$	0.142	$r_2(pnt)$	0.364
Ω_1	8.52	A_1	1.0[b]	i	83.0°	$r_1(side)$	0.142	$r_2(side)$	0.260
Ω_2	2.37	A_2	0.42	q	0.256	$r_1(back)$	0.142	$r_2(back)$	0.293

Notes to TABLE 1

[a]Simultaneous *VB* solutions; *PSHIFT* = −0.00011.
[b]Fixed; for F_1, g_2, A_2, and q determinations, see text.

TABLE 2. Wavelength-dependent parameters.[a]

	V	B
x_1[b]	0.28	0.33
x_2[b]	0.55	0.69
L_1[c]	0.758	0.851
L_2[c]	0.242	0.149
ℓ_{1q}[d]	0.717	0.813
ℓ_{2q}[d]	0.283	0.187
Wt ME(mag)	±0.011	±0.009

Notes to TABLE 2

[a]*VB* solution with ℓ_3's = 0.
[b]Fixed.
[c]Luminosities over 4π steradian.
[d]Lights at quadrature.

RY Per. Subtle circumstellar effects could also contribute to this error.

The only other major parameter not varied in solutions is T_1. We emphasize that changes in T_1 *do* produce small changes in all parameters, including q(phot), and therefore affect parameter errors. If T_1 is uncertain by ±1000 K, then q(phot) changes by ±0.01. We tentatively conclude that q(phot)=0.256±0.011, if the loser fills its Roche lobe. Other mean errors, *including* contributions from the T_1 uncertainty, are: F_1, 0.8; i, 0.3; Ω_1, 0.19; $L_1(V,B)$, 0.009, 0.009; $L_2(V,B)$, 0.003, 0.003. These errors are larger than formal errors from photometric solutions with fixed T_1.

Relative to the Kurucz (1979) grid, the new Kurucz (1992) grid lowered T_2 by 180 K. Other parameter changes were small.

Our solution differs somewhat from that of VHW. Our use of more recent stellar atmosphere grids and a different T_1 may explain most of these differences.

3.1 Absolute Elements

The best available elements of the spectroscopic orbits of both components have been published by Popper (1989). The radial velocity curve of the cool loser poses no serious problem, though most of the lines measured (typically 15 per plate) are rather weak and somewhat diffuse, except for the strong Na I D lines. A circular orbit is plausible and Popper's adopted value is K_2=175.8±1.2 km s^{-1}.

The gainer poses a more difficult problem; its optical line profiles are distorted by the loser as well as by circumstellar matter. Popper finds two He I lines (3819 Å and 4026 Å) most reliable, but even for these, spectra taken at phases 0.7 to 0.8 had to be rejected in order to obtain a circular orbit with K_1=50.1±2.1 km s^{-1}. Hiltner (1946), using plates of much lower dispersion, found only 36 km s^{-1}; Popper believes that Hiltner included the 4471 Å line, which is not reliable (probably because of blends with loser lines). Hydrogen lines, even H8 through H11 which are less affected by the loser, systematically give a much lower velocity range (24 km s^{-1}). Popper says that the hydrogen lines "appear to have an appreciable nonphotospheric component, although asymmetries were not obvious." Our high-dispersion CCD spectra show the circumstellar components clearly; moreover, Hα displays double emission.

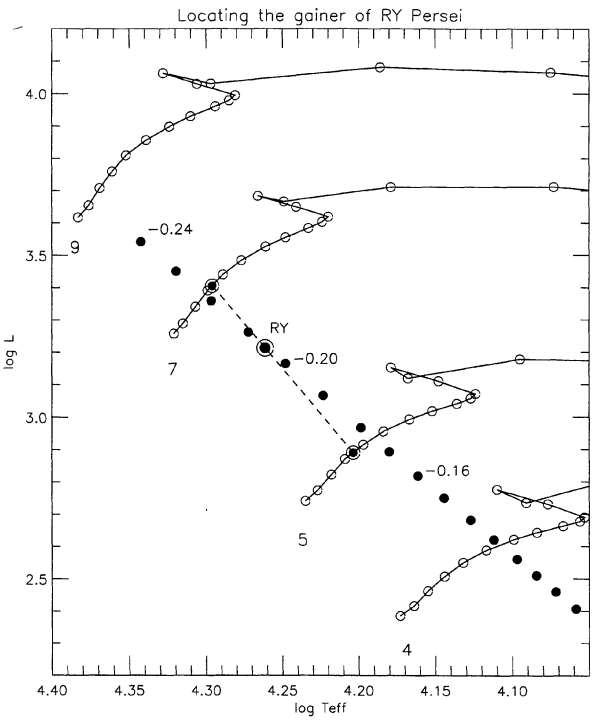

FIG. 6. Location of gainer in the HR diagram.

Popper's value of spectroscopic mass ratio q(spec) $=K_1/K_2$=0.285±0.012. However, in view of the uncertainties in the value of K_1, we prefer the photometric mass ratio q(phot)=0.256 ± 0.011, which gives K_1=45 km s^{-1}, not far below Popper's value. In fact, given their error spreads, q(spec) and q(phot) very nearly overlap. With i=83.0°, we obtain masses M_1=6.25 $M_\odot$, M_2=1.60 $M_\odot$, and separation of the centers A=30.2 $R_\odot$.

3.2 The Gainer

The gainer is distorted by rapid rotation, as the photometric radii in Table 1 show. Its mean radius is R_1=4.06 $R_\odot$, and log g_1 for the mean radius is 4.02. To determine other important parameters, we proceeded as follows: In the latest evolutionary models (Schaller *et al.* 1992), we interpolated in the available tracks for a star of 5 $M_\odot$ and 7 $M_\odot$, respectively, for models with log g_1=4.02. In both cases, these models lie on the very early parts of the main-sequence phase, and correspond to luminosity class V. Their effective temperatures are 16,000 K (for 5 $M_\odot$) and 19,800 K (for 7 $M_\odot$). Then we interpolated linearly between these two models for the value M_1=6.25 $M_\odot$, derived above. As Fig. 6 shows, the interpolated model for the gainer corresponds to a mean effective temperature T_1=18,250 K, and to a luminosity L_1=1630 $L_\odot$.

The only other estimate of mean gainer effective temperature comes from VHW, who assumed 20,700 K. Their value was derived by scaling up the value of an adopted "observed" temperature, namely 18,800 K, which in turn was based on the estimated spectral type of B3 V, published by Hill *et al.* (1975). However, those authors also give another

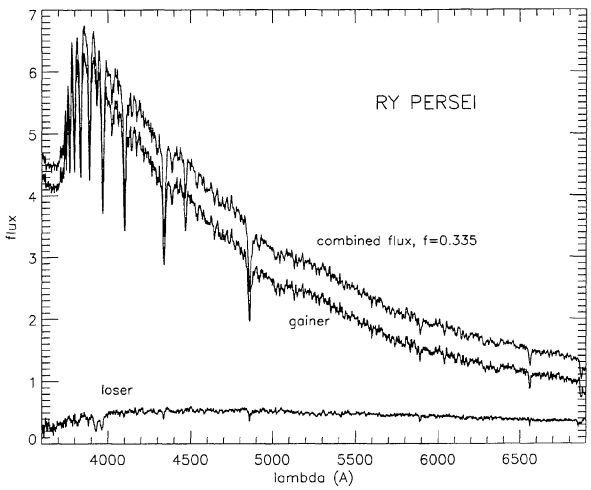

FIG. 7. Optical spectra of the loser, gainer, and their combined light (bottom to top). The fluxes are expressed in units of 10^{-12} ergs cm^{-2} s^{-1} Å^{-1}.

estimate, B4 V. Popper (1989) gives B5 in the text (p. 604) and B4 in the final table (p. 620). One would then prefer to accept B4 V as a mean value, corresponding to 17,000 K, which agrees with our direct spectroscopic determination. The latter is, moreover, much more accurate, since it is based on a careful fitting of our observed spectra to state-of-art non-LTE atmospheric models and spectra developed by Hubeny (1988 and subsequent developments). From the above numbers and from Fig. 6, it is obvious that 20,700 K is too high for a star of 6.25 $M_\odot$; similarly, our spectroscopic data rule out the value of 18,800 K for the observed spectrum.

The diagram of evolutionary tracks in Fig. 6 also provides a good estimate of the intrinsic value of the color $(B-V)_0$, as follows: Böhm-Vitense (1981) published a table relating this quantity to $T_{\rm eff}$. Her table was used to plot the sequence of filled circles in the Fig. 6 . That it passes exactly through the locus representing the gainer is partly an artifact, since the luminosity was calculated assuming $R_1=4.06R_\odot$. Nevertheless, $(B-V)_0=-0.205$ mag must be close to the correct value, and the acceptable range is narrow, about ± 0.015 mag. Napiwotzki *et al.* (1993) provided another relation between $(B-V)_0$ and $T_{\rm eff}$ (on p. 658); from it, we get $(B-V)_0=-0.200$ mag. Finally, from data provided by Kurucz (1996), we interpolate, for $\log g_1=4.0$, $(B-V)_0=-0.193$ mag.

We now discuss the observed spectral characteristics. Figure 7 shows observed optical spectra: combined spectrum at phase 0.3351, loser spectrum at totality (phase 0.0024), and subtracted spectrum, representing approximately the gainer. Since only a low-resolution IDS loser spectrum is available, we are plotting all the spectra consistently at the same resolution.

The most reliable determination of the observed (i.e., approximately equatorial) temperature comes from the fitting of our CCD high-dispersion spectra in the interval 3500 through 4200 Å. This fit is independent of interstellar reddening over a wide range of E$(B-V)$, and the flux contribution by the loser is small, flat, and virtually negligible. Only temperature values between 17,000 and 17,500 K are acceptable, and the effective value of $\log g_1=3.7\pm 0.1$ is also fairly narrowly fixed. This value, distinctly lower than 4.02 derived above, confirms that we are observing flux predominantly from the equatorial region of the rapidly rotating gainer. Indeed, the observed value is close to that expected if we take into account centrifugal acceleration.

As mentioned above, the photometric ratio of observed to synchronized velocity of rotation is $F_1\approx 9.8$, from which we get the equatorial rotational velocity $V_{\rm rot}\approx 292$ km s^{-1}. The spectroscopic determination gives 212 km s^{-1} (Etzel & Olson 1993). If the observed spectrum is due mainly to the equatorial bulge, we then expect an effective value of $\log (g_{\rm grav}-g_{\rm rot})=3.78$, in good agreement with observation.

The optical spectral region between 4000 and 6000 Å is well fitted by a synthetic spectrum corresponding to $T\approx 17{,}000$ K. This determination carries less weight, though, since, as Fig. 7 shows, the contribution by the loser plays an increasing role, and we do not know if fluxes derived for the latter from the totality spectrum can be applied at other orbital phases. The ultraviolet *IUE* spectra pose a different problem: here the color excess, E$(B-V)$, plays an important role. In a number of Algol systems, this value was surprisingly well determined from the interstellar bump at 2200 Å (Dobias & Plavec 1989), in spite of frequent warnings that this procedure is not reliable. In RY Per, this procedure offers rather crude limits, since in all spectra the relevant region is extremely noisy. We can only say that values of the excess below 0.15 mag do not remove the bump, while values above 0.20 mag tend to create spurious emissions.

We proceed as follows: The observed color of the gainer, derived from photometry, is $(B-V)=-0.014$ mag. This value, we presume, corresponds to the observed $T_1=17{,}200$ K. We will use the tables by Kurucz (1996) to upgrade it to the anticipated mean temperature, 18,250 K. The correction is -0.012 mag, so we adopt $(B-V)=-0.026$ mag. From the graph in Fig. 6, we derived $(B-V)_0=-0.205$ *mag, so we conclude that* $E(B-V)\approx 0.18$ mag.

Now we attempt to derive the absolute visual magnitude of the gainer. The combined light of both components, determined from phases just outside primary eclipse (in order to minimize the reflected light), is $V_c=8.559$ mag, $B_c=8.658$ mag, and $U_c=8.217$ mag. From these values we subtract the light of the loser as measured during totality ($V_2=10.220$, $B_2=10.865$, $U_2=11.085$ mag); we find that the loser contributes 22% to the combined light in the V band. Thus the observed magnitude of the gainer is $V_1=8.824$ mag. Next, we apply the dereddening correction corresponding to the color excess of 0.18 mag, namely 0.558 mag. Thus the corrected gainer magnitude is $V_1=8.266$ mag. We think that this value should again be corrected for the temperature difference of about 1000 K. According to Kurucz' tables, the correction is near -0.11 mag, so that we estimate that the gainer should properly be represented by an observed visual magnitude of $V_1=8.16$ mag.

From the interpolation in Fig. 6, explained above, we obtained $\log L_1=3.212$; adopting the absolute bolometric magnitude of the Sun to be $+4.75$ (Zombeck 1990), we get the absolute bolometric magnitude of the gainer as -3.28 mag.

TABLE 3. Estimated absolute system parameters.[a]

Parameter	Star 1	Star 2
$M/M_\odot$	6.25±0.16	1.60±0.10
$R/R_\odot$	4.06±0.14	8.10±0.17
log $L/L_\odot$	3.21	1.98
M_{bol}	−3.28	−0.2
log g (cgs)	4.02	2.83
v_{syn} (km s^{-1})	30.	60.
M_V	−1.46	0.04
$E(B-V)$	0.18	...
A_V	0.56	...
$d(pc)$	840	...

Notes to TABLE 3

[a]Other parameters are in Tables 1 and 2.

The bolometric correction at 18,250 K is about −1.82 mag (Kurucz 1996). Thus the absolute visual magnitude of the gainer is near −1.46 mag. We derive the probable distance to RY Per to be about 840 pc, distance modulus $m-M=9.62$ mag.

We are painfully aware that these calculations, from the observed data to the presumably correct data for a nonrotating star, are very crude and tentative. A deep analysis of the parameters of a rapidly rotating star is needed. We must, however, caution that—even if such treatment were available—we are far from sure that it would be applicable to RY Per. There is no doubt that rapid rotation is the result of mass transfer (Plavec 1970). However, it is not clear if the transferred material settles quietly upon the gainer, forming a normal atmosphere of a genuine rotational ellipsoid. The high-dispersion *IUE* ultraviolet spectra, especially those taken with the SWP (short-wavelength) camera show a clear deviation from the gainer parameters derived from the optical and near-infrared photometry and spectroscopy. There seems to be a continuous opacity steadily increasing towards the shorter wavelength, starting at least near 1450 Å but quite possibly already at a longer wavelength. Moreover, the FUV absorption lines–perhaps with a very few exceptions–indicate a much lower rotational velocity, definitely below 100 km s^{-1}. The correct model would probably include a circumstellar disk only loosely attached to the gainer, with its boundary layer playing the role of a pseudo-photosphere as proposed by Shore & King (1986). These masses and dimensions place RY Per near the boundary between cases where the accretion disk is stable and cases where it should be only transient. The problem of the character of the circumstellar structures is wide open.

We plan to study this problem using new high-dispersion *IUE* spectra obtained by G. J. Peters and Plavec.

There is no doubt that circumstellar matter plays an important role in the spectroscopic aspects of RY Per. The most convincing evidence for circumstellar material is provided by the relatively intense ultraviolet emission lines observed when the gainer is totally eclipsed—that is, coming from a volume much larger than that occulted by the larger loser. We discuss these emission lines in a later section, after we examine the properties of the loser.

3.3 The Loser

Observations at totality yield the following observed magnitudes and loser colors: $V=10.220$, $B=10.865$, $U=11.085$, $(B-V)=0.645$, $(U-B)=0.220$. By applying the corrections corresponding to the adopted color excess $E(B-V)=0.18$ mag, we obtain the following observed but dereddened values: $V_2=9.662$ mag, $B_2=10.127$ mag, $U_2=10.217$ mag, $(B-V)_2=+0.465$ mag, $(U-B)_2=+0.089$ mag. From the new Kurucz (1996) models, the above value of $(B-V)_2$ implies $T_2=6460$ K, while according to Böhm-Vitense (1981), the value of the effective temperature is 6470 K. Schmidt-Kaler's table for giants (luminosity class III) suggests $T_2\approx 6370$ K, and spectral type F6 III. The same value for T_2 results when the formula (11) in Napiwotzki *et al.* (1993) is applied. All these results are based on the $(B-V)$ color. The $(U-B)_2$ value derived above, if taken literally, combined with the value of $\log g_2=2.8$ derived from the absolute dimensions, does not have any corresponding value of effective temperature over the range $5500 < T_{\rm eff} < 7500$ K. As we remarked in Sec. 3.1, the U magnitudes are probably disturbed. The photometric solution gives $T_2=6250$ K, which, after Schmidt-Kaler, corresponds to spectral type F7.

The resolution of the loser spectrum obtained at totality is too low for spectral line analysis, but a comparison of the continuous flux distribution with the spectral scans published by Gunn & Stryker (1983) suggests a spectral type of F9 and no later than G0, definitely not G2, G4, or even G8 as listed in Yoon *et al.* (1994). Thus the discrepancy between the "photometric" spectral type (F6–F7) and the "spectroscopic" spectral type (F9–G0) may exist in the sense pointed out by Yoon *et al.*, but is far less striking than they indicated.

By using the distance modulus of m-$M=9.62$ mag derived for the gainer, we find that the absolute visual magnitude of the loser should be near zero; the value actually derived is $M_{v,2}=+0.04$ mag. Thus, the loser appears to be about an F7 III-II giant despite its rather low mass of only 1.6 $M_\odot$—a clear sign of the typical Algol-type evolution of an interacting binary with considerable mass transfer between the components.

Relevant parameters are listed in Table 3.

4. CIRCUMSTELLAR EMISSION

The best evidence for mass transfer is provided by the emission-line ultraviolet spectrum observed during and near the total eclipse. Totality emission lines are listed in Table 4. In Table 5, we list all the spectra used in this paper. Phases between 0.945 and 0.055 correspond to the primary eclipse; among them, phases between 0.993 and 0.007 correspond to the total eclipse. Emission lines show up already during the partial ingress; specifically, they were observed in the SWP camera at phase 0.978. Three SWP spectra are nearly identical with the lowest continuous flux, namely those taken at phases 0.9969, 0.9993, and 0.0014. The SWP spectrum at 0.0167, clearly taken in partial eclipse, still shows the emission lines. Among the LWP spectra, again three were taken in totality, namely those at phases 0.9925, 0.0045, and 0.0061.

TABLE 4. Emission lines observed in totality.

λ Å	λ_0 Å	f_{peak} $10^{-13} erg/cm^2/s/Å$	emis. meas. $10^{-12} erg/cm^2/s$	ident	rem.
1242.2	1238.8, 1242.8	21.9	17.5	N V (1)	a
1297.4	1298.9	5.5	7.8	Si III (4)	b
1335.2	1334.5, 1335.7	3.3	2.6	C II (1)	c
1344.9	1344.3, 1344.9	4.0	2.4	P III (1)	d
1392.8	1393.7	15.7	10.0	Si IV (1)	e
1403.6	1402.7	15.1	8.0	Si IV (1)	e
1534.2	1533.4	2.5	1.3	Si II (2)	f
1549.8	1548.2, 1550.8	4.1	3.5	C IV (1)	g
1672.6	1670.8	2.2	1.6	Al II (2)	h
1724.4	1725.0	2.7	1.5	Al II (6)?	i
1852.9	1854.7	8.4	8.0	Al III (1)	j
1865.1	1862.8	7.6	6.0	Al III (1)	j
1895.4	1895.5	6.6	7.6	Fe III (34)	
1914.7	1914.1	5.7	5.9	Fe III (34)	j
1928.6	1926.3	6.1	7.2	Fe III (34)	j
1986.2	1987.5 etc	6.2	7.8	Fe III (50)	k
2056.6	2056.1 etc	7.0	7.2	Fe III (71)	k
2077.0	2079.0 etc	8.0	8.2	Fe III (48)	k
2801.4	2795.5, 2802.7	2.7	1.5	Mg II (1)	l

Notes to TABLE 4

[a]surprisingly strong; [b]broad blend, contribution by Si II (3) probably small; [c]low V peak in blend; [d]R peak in double; [e]sharp, strong; [f]very low; [g]surprisingly weak: underabundance of C; [h]low, narrow; [i]very narrow, ID tentative; [j]a pair only partly resolved; [k]noisy region, ID very tentative, probably blends of more Fe III multiplets; [l]unusually weak.

TABLE 5. Spectra used for this article.

phase	epoch	HJD	exp(s)	instrument	obs.
0.0014	633	46000.4453	3600	SWP 24308 LLO	P
0.0024	461	44819.9180	400	IDS 1m, BR	D,S
0.0045	596	45746.5156	1200	LWP 2784 LLO	E
0.0061	633	46000.4805	1200	LWP 4653 LLO	P
0.0073	952	48189.9648	3000	SWP 39946 LLO	Po
0.0102	633	46000.5078	1800	SWP 24309 LLO	P
0.0130	633	46000.5273	720	LWP 4654 LLO	P
0.0155	952	48190.0195	1500	SWP 39947 LLO	Po
0.0167	633	46000.5508	900	SWP 24310 LLO	P
0.0199	633	46000.5742	360	LWP 4655 LLO	P
0.0530	837	47400.9688	6000	HAM high-disp	P,C
0.1296	461	44820.7930	90	LWR 11236 LLO	P
0.1301	461	44820.7969	130	SWP 14645 LLO	P
0.3327	360	44128.9648	240	IDS 3m, BR	P,K
0.3351	471	44890.8398	300	IDS 3m, BRI	P,W
0.4051	884	47725.9727	6000	HAM high-disp	P,C
0.4791	360	44129.9727	240	IDS 3m, BR	P,K
0.5245	789	47074.7539	6000	HAM high-disp	P,C
0.6568	354	44090.0117	400	IDS 1m, BR	D,S
0.8918	946	48154.8555	4800	LWP 18834 LHI	P
0.8965	946	48154.8867	120	SWP 39665 LLO	P
0.9001	946	48154.9102	90	LWP 18835 LLO	P
0.9120	522	45244.8398	300	IDS 3m, BRI	P,W
0.9250	946	48155.0820	8100	SWP 39667 LHI	P
0.9780	951	48189.7656	480	SWP 39943 LLO	Po
0.9852	951	48189.8125	1500	SWP 39944 LLO	Po
0.9888	595	45746.4102	2400	SWP 22273 LLO	E
0.9925	595	45746.4336	1200	LWP 2783 LLO	E
0.9969	951	48189.8945	4800	SWP 39945 LLO	Po
0.9993	595	45746.4805	4500	SWP 22274 LLO	E

Notes to TABLE 5

Instruments: *IUE* spectra: SWP: short-wavelength camera, LWP: long-wavelength camera; LLO: large aperture, low dispersion; LHI: large aperture, high dispersion. Optical spectra, taken at Lick Observatory: IDS: low-resolution scanner, BRI indicate spectral regions covered; HAM: high-dispersion CCD spectrum, Hamilton spectrograph.—Observers: C=C.R. Cliff, D: J.J. Dobias, E: P.B. Etzel, K: C.D. Keyes, P: M.J. Plavec, Po: R.S.Polidan, S: R.P. Stone, W: Janet L. Weiland.

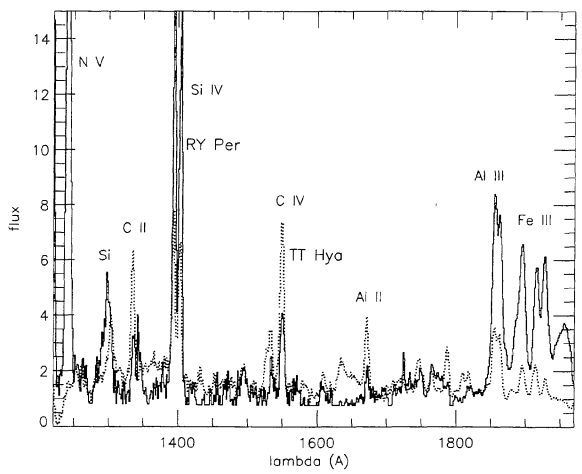

FIG. 8. Far ultraviolet (*IUE*-SWP) totality spectra of RY Per (heavy line) and TT Hya. The fluxes are expressed in units of 10^{-13} ergs cm^{-2} s^{-1} Å^{-1}.

In Fig. 8, we show the SWP spectrum (phase 0.9993) that shows the strongest emission lines, and compare it with the totality spectrum of TT Hydrae as studied by Plavec (1988). In general, the emissions in RY Per are stronger (although a comparison of directly observed fluxes would not show it; in contrast to RY Per, TT Hya suffers virtually no interstellar extinction). A closer inspection shows two significant differences: (1) The emissions in RY Per indicate a higher ionization level: Fe III lines are strong, while Fe II lines cannot be recognized, at least not at this low dispersion; Si II lines are weaker than usual in other Algols; the Al III doublet is much stronger than Al II; the resonance multiplet of P III (1) shows near the C II 1335 Å line like in no cooler Algols; and, above all, N V is extremely strong, while it does not exist in TT Hya. (2) However, there is a very significant exception: the C IV doublet is much weaker than in TT Hya. This, along with the weakness of C II, suggests that carbon is significantly underabundant, while nitrogen is overabundant compared to normal stars, as is to be expected in massive Algols, and as was already pointed out by Polidan & Wade (1992).

The LWP totality spectra show extremely low flux with no conspicuous emissions from 2200 Å longward. The Mg II resonance doublet is extremely weak, and there is no trace of the rich Fe II spectrum which so strikingly elevates the flux in TT Hya. This reconfirms the fact that the general level of ionization is significantly higher in RY Per. Plavec (1989) discussed the more general aspects of ionization levels in circumstellar envelopes around Algols, and pointed out that a correlation seems to exist between the effective temperature of the gainer and the ionization level; however, much more work is needed before we can understand the circumstellar envelopes in Algols, and RY Per certainly is an important system for this purpose.

The emissions observed at totality represent only one aspect of circumstellar matter. Important information is contained in the continuous flux distribution and in the absorption lines observed in the ultraviolet at high dispersion with the *IUE* satellite by G. J. Peters and Plavec.

Before we could address those topics, it was necessary to derive a reasonably reliable picture of the binary system, which we attempted in the present paper.

We thank Dr. Dan Popper for supplying the Popper-Dumont *UBV* photometric observations, Dr. Gene Milone and his Calgary colleagues for supplying *VBU* fluxes from the new Kurucz (1992) atmosphere grid, and Dr. Robert Kurucz for supplying colors and bolometric corrections for his 1992 atmosphere grid. Dr. Paul Etzel contributed many helpful suggestions. Dr. Ivan Hubeny provided his valuable codes for computing stellar atmosphere models and synthetic spectra. We also wish to thank all participating observers, and the directors and staffs of the Lick and *IUE* Observatories. Jeannette Barnes provided assistance in formatting tables. This work was partially supported by NASA ADP Grant No. NAG 5-2653 to Plavec.

REFERENCES

Böhm-Vitense, E 1981, Ann. Rev. Astron. Aph., 19, 295
Carbon, D.F., & Gingerich, O. 1969, in Theory and Observation of Normal Stellar Atmospheres, edited by O. Gingerich (MIT, Cambridge)
Dobias, J. J., & Plavec, M. J. 1989, Space Sci. Rev., 50, 340
Etzel, P. B., & Olson, E. C. 1993, AJ, 106, 1200
Gunn, J. E., & Stryker, L. L. 1983, ApJS, 52, 121
Hill, G., Hilditch, R. W., Younger, F., & Fisher, W. A. 1975, MNRAS, 79, 131
Hiltner, W. A. 1946, ApJ, 104, 396
Hubeny, I. 1988, Comput. Phys. Commun., 52, 103
Kurucz, R. L. 1979, ApJS, 40, 1
Kurucz, R. L. 1992, in Stellar Populations of Galaxies, IAU Symposium 149, edited by B. Baybuy and A. Renzini (Kluwer, Dordrecht), p.225
Kurucz, R. L. 1996, private communication
Napiwotzki, R., Schönberner, D., & Wenske, V. 1993, A&A, 268, 653
Plavec, M. J. 1970, in Stellar Rotation, edited by A. Slettebak (Reidel, Dordrecht), p. 133
Plavec, M. J. 1987, Publ. Astron. Inst. Czech. Ac. Sci., 70, 193
Plavec, M. J. 1988, AJ, 96, 755
Plavec, M. J. 1989, Space Sci. Rev., 50, 95
Polidan, R. S., & Wade, R. A. 1992, in Evolutionary Processes in Interacting Binary Systems, edited by Y. Kondo, R. F. Sistero, and R. S. Polidan (Kluwer, Dordrecht), p. 351
Popper, D. M. 1989, ApJS, 71, 595
Popper, D. M., & Dumont, P. J. 1977, AJ, 82, 216
Schaller, G., Schaerer, D., Meynet, G., & Maeder, A. 1992, A&AS, 96, 269
Shore, S. N., & King, A. R. 1986, A&A, 154, 263
Schmidt-Kaler, Th. 1982, in Landolt-Börnstein, Bd. 2b, 453
Stagg, C. R. 1992, private communication
Van Hamme, W., & Wilson, R. E. 1986, AJ, 92, 1168
Van Hamme, W. 1993, AJ, 106, 2096
Wilson, R. E. 1979, ApJ, 234, 1054
Wilson, R. E. 1992, Documentation of Eclipsing Binary Computer Model (University of Florida, Gainesville, FL)
Yoon, T. S., Honeycutt, R. K., Kaitchuck, R. H., & Schlegel, E. M. 1994, PASP, 106, 239
Zombeck, M.V. 1990, Handbook of Space Astronomy and Astrophysics, 25